

A *NUSTAR* OBSERVATION OF THE GAMMA-RAY-EMITTING X-RAY BINARY AND TRANSITIONAL MILLISECOND PULSAR CANDIDATE 1RXS J154439.4–112820

SLAVKO BOGDANOV

Columbia Astrophysics Laboratory, Columbia University, 550 West 120th Street, New York, NY 10027, USA

Submitted to the Astrophysical Journal Letters on August 10, 2021

ABSTRACT

I present a 40 kilosecond *Nuclear Spectroscopic Telescope Array* (*NuSTAR*) observation of the recently identified low-luminosity X-ray binary and transitional millisecond pulsar (tMSP) candidate 1RXS J154439.4–112820, which is associated with the high-energy γ -ray source 3FGL J1544.6–1125. The system is detected up to ~ 30 keV with an extension of the same power-law spectrum and rapid large-amplitude variability between two flux levels observed in soft X-rays. These findings provide further evidence that 1RXS J154439.4–112820 belongs to the same class of objects as the nearby bona fide tMSPs PSR J1023+0038 and XSS J12270–4859 and therefore almost certainly hosts a millisecond pulsar accreting at low luminosities. I also examine the long-term accretion history of 1RXS J154439.4–112820 based on archival optical, ultraviolet, X-ray, and γ -ray light curves covering the past \sim decade. Throughout this period, the source has maintained similar flux levels at all wavelengths, which is an indication that it has not experienced prolonged episodes of a non-accreting radio pulsar state but may spontaneously undergo such a state transformation in the future.

Subject headings: pulsars: general — stars: neutron — X-rays: binaries

1. INTRODUCTION

The recent discovery of three millisecond pulsar (MSP) binary systems that alternate between clearly distinguishable rotation- and accretion-powered states have revealed a new aspect of compact binaries containing neutron stars (Papitto et al. 2013; Patruno et al. 2014; Bassa et al. 2014). In their accreting states, these objects show rapid optical/UV variability and a bimodal X-ray variability pattern (Linares et al. 2014; de Martino et al. 2013; Bogdanov et al. 2015) — the X-ray flux switches rapidly between two distinct high and low “modes” that differ by a factor of 6–10. In addition, these systems constitute the only γ -ray-emitting variety of low-mass X-ray binary; both confirmed nearby transitional MSPs, PSR J1023+0038 and XSS J12270–4859, are bright *Fermi* LAT sources even when accreting¹. The unique combination of observational characteristics offers a fairly straightforward way to identify additional objects that belong to this class.

In Bogdanov & Halpern (2015), we examined the X-ray and optical/UV properties of the bright *ROSAT* source 1RXS J154439.4–112820, which is positionally coincident with the high-energy γ -ray source 3FGL J1544.6–1125 (Stephen et al. 2010; Masetti et al. 2013). The variability and spectral properties of this system were found to be essentially identical to those observed from the nearby transitional millisecond pulsar binaries PSR J1023+0038 (Bogdanov et al. 2015) and XSS J12270–4859 (de Martino et al. 2013). The available observational evidence points to 1RXS J154439.4–112820 most probably being a transitional MSPs in a low-luminosity accreting state, making it only the fourth such system to be identified.

Two of the transitional MSPs, XSS J12270–4859

and PSR J1824–2452I, are currently in a dormant, accretion-disk-free state (Bassa et al. 2014; Roy et al. 2015; Bogdanov et al. 2014a; Papitto et al. 2013), leaving only PSR J1023+0038 and 1RXS J154439.4–112820 available for further detailed studies of the accreting state. At present, the underlying physical processes responsible for the observed phenomenology, especially the rapid X-ray mode switching and unexpectedly bright high-energy γ -ray emission associated with the accreting state, are poorly understood. In light of the transitory nature of the accreting state, it is therefore crucially important to investigate each system extensively at all wavelengths before a transformation to a possibly prolonged non-accreting episode (lasting years to decades).

On-going multiwavelength studies of PSR J1023+0038 in its present accreting state (Archibald et al. 2015; Deller et al. 2015; Bogdanov et al. 2015) are revealing new information regarding the accretion and jet production processes that operate in transitional MSPs. In this paper, I present complementary results on 1RXS J154439.4–112820 including a target of opportunity hard X-ray observation using the *Nuclear Spectroscopic Telescope Array* (*NuSTAR*), which further confirm the similarities of this system with transitional MSPs. I also investigate the broad band spectral energy distribution and long-term variability of the system, which further strengthen the classification of this system as a transitional MSP. This work is organized as follows. In §2, I summarize the *NuSTAR* observation and data analysis. In §3, I describe the X-ray spectroscopic analysis, while in §4 I focus on the hard X-ray variability. In §5 I discuss the broad band spectral energy distribution of 1RXS J154439.4–112820. I offer a discussion in §6 and conclusions in §7.

2. OBSERVATION AND DATA ANALYSIS

The 1RXS J154439.4–112820 system was observed with *NuSTAR* (Harrison et al. 2013) on 23 March 2015

¹ For the third transitional MSP, PSR J1824–2452I, which is situated in the globular cluster M28, its γ -ray emission cannot be reliably disentangled from the 11 other radio MSPs in the cluster.

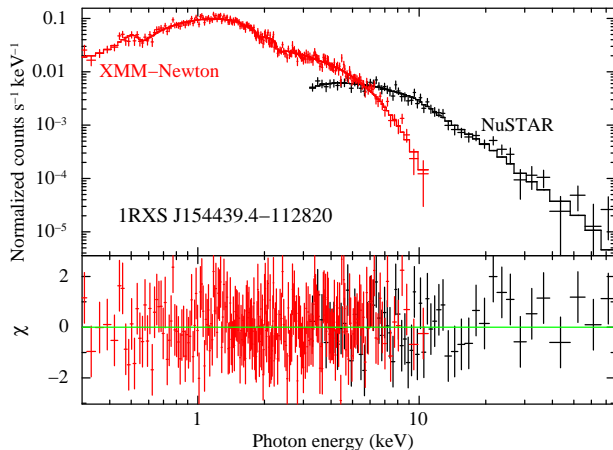


FIG. 1.— *NuSTAR* FPMA+FPMB (black) and *XMM-Newton* MOS1+MOS2 (red) spectra of 1RXS J154439.4–112820 jointly fitted with an absorbed power-law model. The bottom panel shows the best fit residuals expressed in terms of σ with error bars of size unity. See text for best fit parameters.

(ObsID 90001007) in a 40 ks effective on-source exposure obtained through the Director’s Discretionary Program. *NuSTAR* is the first focusing hard X-ray telescope, with sensitivity over the 3–79 keV energy range. It consists of two co-aligned telescopes, which use grazing-incidence mirror assemblies to focus hard X-rays onto two Focal Plane Modules, FPMA and FPMB.

The data were processed using the `nupipeline` script in NuSTARDAS and the images, spectra, and light curves were generated using the `nuproducts` task. 1RXS J154439.4–112820 is the only hard X-ray source within the telescope field of view and is detected with high significance up to ~ 30 keV. For both the spectroscopic and time variability analyses, the source counts were extracted from a circular region of radius $60''$ (which encircles $\sim 80\%$ of the total source energy) centered on the optical position reported in Bogdanov & Halpern (2015). The background was taken from a $60''$ radius source-free region.

3. X-RAY SPECTROSCOPY

I conducted a spectral analysis in XSPEC version 12.8.2 (Arnaud 1996). To maximize the photon statistics, the FPMA and FPMB spectra and response functions were combined using the `addascaspec` command in FTOOLS. Based on the results from the *XMM-Newton* spectroscopy presented in (Bogdanov & Halpern 2015), the *NuSTAR* FPMA and FPMB spectra were fitted with an absorbed power-law assuming the `tbabs` interstellar absorption model and chemical abundances from Wilms et al. (2000). This produces a best fit with hydrogen column density of $N_{\text{H}} \leq 1.3 \times 10^{22} \text{ cm}^{-2}$, spectral photon index $\Gamma = 1.68 \pm 0.06$, an unabsorbed 3–79 keV flux of $F_X = (6.6 \pm 0.4) \times 10^{-12} \text{ erg cm}^{-2} \text{ s}^{-1}$, and $\chi^2_{\nu} = 1.14$ for 156 degrees of freedom. Owing to the hard response of *NuSTAR*, the fit is insensitive to the value of N and only a crude upper limit is obtained. To further refine the spectral parameters, I also conducted a joint fit to the *XMM-Newton* and *NuSTAR* data. The resulting best fit with an absorbed power-law gives $N_{\text{H}} = (1.7 \pm 0.1) \times 10^{21} \text{ cm}^{-2}$, $\Gamma = 1.67 \pm 0.02$, and

$F_X = (8.4 \pm 0.2) \times 10^{-12} \text{ erg cm}^{-2} \text{ s}^{-1}$ (0.3–79 keV), with $\chi^2_{\nu} = 0.96$ for 471 degrees of freedom. All uncertainties quoted are at a 90% confidence level. No adjustment to the cross-normalizations between the two data sets was required. As apparent from Figure 1, the spectral continuum shows no evidence for a break or turn-over within the *NuSTAR* band.

I also explored the possibility of spectral variability by computing the hardness ratio variations as a function of count rate. There are no statistically significant differences in hardness between the high and low flux modes, which is consistent with the result from the *NuSTAR* data of PSR J1023+0038 in its accreting state (Tendulkar et al. 2014).

4. HARD X-RAY VARIABILITY

A total background-subtracted hard X-ray light curve was generated by combining the emission from FPMA and FPMB. As shown in Bogdanov & Halpern (2015), the soft X-ray emission exhibits rapid switching between two flux modes, with ingress and egress durations lasting of order 10 s. Despite the much lower count rate compared to the 0.3–10 keV *XMM-Newton* light curve, the rapid variability is still clearly apparent. The 3–79 keV light curve of 1RXS J154439.4–112820, binned at 100 s resolution, is shown in Figure 2. While the source spends most of the time at a high flux level ($\sim 0.1 \text{ counts s}^{-1}$), multiple instances of low flux levels (reaching down to $\sim 0.01 \text{ counts s}^{-1}$) are evident. At the 100 s bin resolution some short-lived low modes are likely averaged with the high modes occurring within the same time bin. A Kuiper’s test for time variability on the unbinned time series, corrected for good time intervals by removing gaps in exposure, gives a 9×10^{-16} ($\approx 7.9\sigma$) probability that a distribution with a constant count rate would exhibit the observed level of non-uniformity. Due to the relatively low source count rate, the unknown orbital period, as well as known calibration issues with the *NuSTAR* on-board clock, I have not attempted a periodicity search.

5. LONG-TERM BROADBAND BEHAVIOR

PSR J1824–2452I in M28 was observed to be in a very faint ($L_X \approx 10^{32} \text{ erg s}^{-1}$) non-accreting state in 2002 (Becker et al. 2003) and a low-luminosity ($L_X \approx 3 \times 10^{33} \text{ erg s}^{-1}$) accreting state in 2008 (Bogdanov et al. 2011). The optical brightness between these two states differed by ~ 2 magnitudes (Pallanca et al. 2013). As reported in Patruno et al. (2014), the re-appearance of the accretion disk in PSR J1023+0038 was accompanied by a ~ 3.5 magnitude increase in UV brightness and a ~ 20 -fold rise in X-ray luminosity. Similarly, in the state transition of XSS J12270–4859 (Bassa et al. 2014), the transformation from an accreting state to a radio pulsar state was signaled by a decrease in X-ray luminosity by a factor of ~ 10 and decline in UV and optical brightness by ~ 3 and ~ 2 magnitudes, respectively. For PSR J1023+0038, the return of the accretion disk also coincided with a factor of ~ 5 enhancement in high-energy γ -ray luminosity as seen by *Fermi* LAT (Stappers et al. 2014). The disappearance of the accretion disk in XSS J12270–4859 was associated with a ~ 2 -fold decline in γ -ray flux (Yi & Wang 2015).

As 1RXS J154439.4–112820 closely resembles these

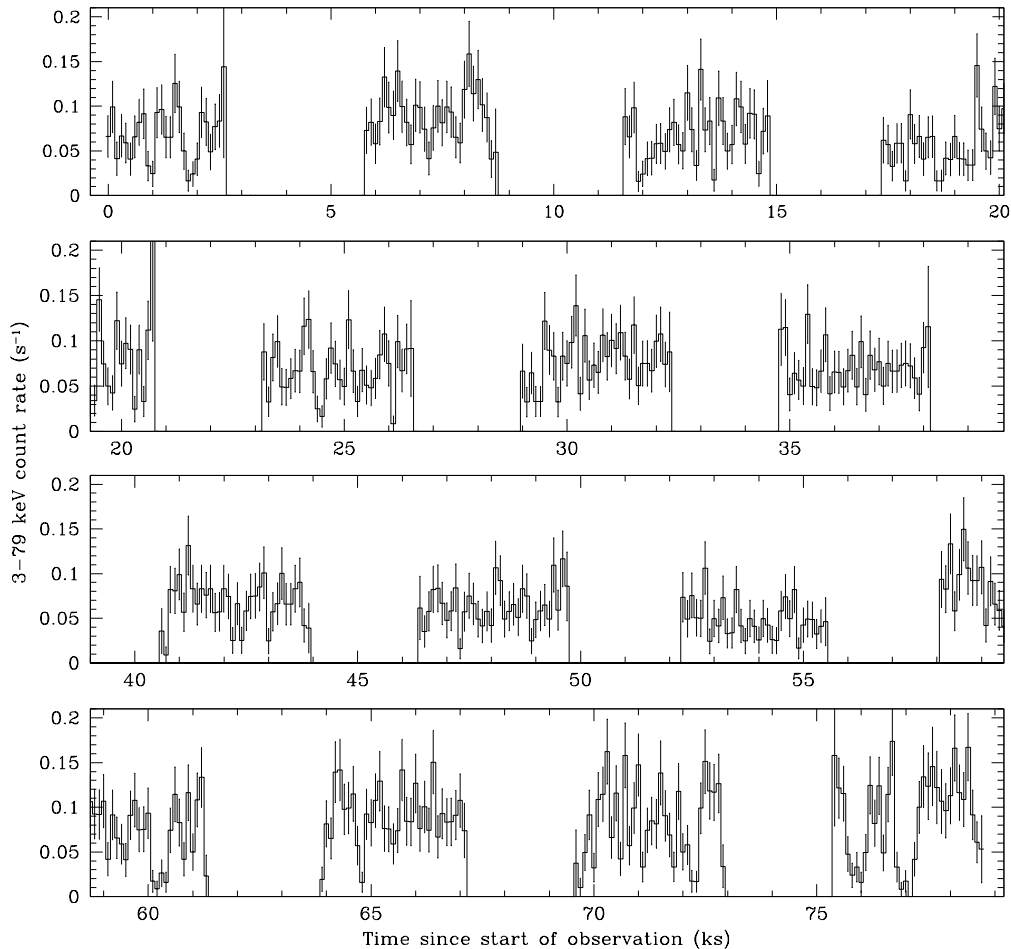


FIG. 2.— *NuSTAR* FPMA+FPMB 3–79 keV background-subtracted light curve of 1RXS J154439.4–112820 binned at a 100 s resolution. The regular ~ 3 ks gaps are due to Earth occultation. Note the occasional short-lived rapid drops in count rate, especially towards the end of the observation.

transitional MSP systems, it may have also experienced transitions to and from a disk-free state in the past. Examination of archival data is particularly valuable in this regard, considering that both PSR J1824–2452I (in 2008–2009 Pallanca et al. 2013; Linares et al. 2014) and XSS J12270–4859 (in 2012 Bassa et al. 2014) were uncovered retroactively to have undergone state transitions in archived data sets. Prompted by this possibility, I have investigated the optical/UV, X-ray, and γ -ray variability of 1RXS J154439.4–112820 on time scales of years. For this purpose, I use publicly available data from the Catalina Real-time Transient Survey (Drake et al. 2009), *Swift* XRT and UVOT, and *Fermi* LAT data. Figure 3 shows the lightcurves from these data sets, which are described below.

5.1. Catalina Real-time Transient Survey

The Catalina Real-time Transient Survey (CRTS Drake et al. 2009) acquires unfiltered exposures of the sky away from the Galactic plane that usually reach equivalent *V* filter of ~ 19 –20. The CRTS archive includes 324 observations of 1RXS J154439.4–112820 spanning from late 2005 to late 2013. Removing points with magnitude errors greater than 0.2 results in 260 in-

dividual exposures.

5.2. *Swift* UVOT and XRT

The error ellipse of 3FGL J1544.6–1125 has been targeted with *Swift* once in 2006 and 2007, twice in 2012, and on six occasions in 2015.

The *Swift* UVOT data include four exposures with the UVW1, two with the UVW1, three with the UM2, and three with the U filter. The photometric measurements and associated uncertainties were extracted with the `uvotsource` task in FTOOLS, using a source extraction region of radius $5''$ centered on the optical position given in Bogdanov & Halpern (2015).

The 12 *Swift* XRT observations were all obtained in photon counting (PC) mode. The 0.3–10 keV light curves were extracted using the `xrtpipeline` command in FTOOLS. The counts were grouped adaptively to ensure that each time bin contained at least 20 counts.

5.3. *Fermi* LAT

To investigate the high-energy γ -ray variability of 1RXS J154439.4–112820 on long timescales, I have retrieved all Pass 8 *Fermi* Large Area Telescope (LAT)

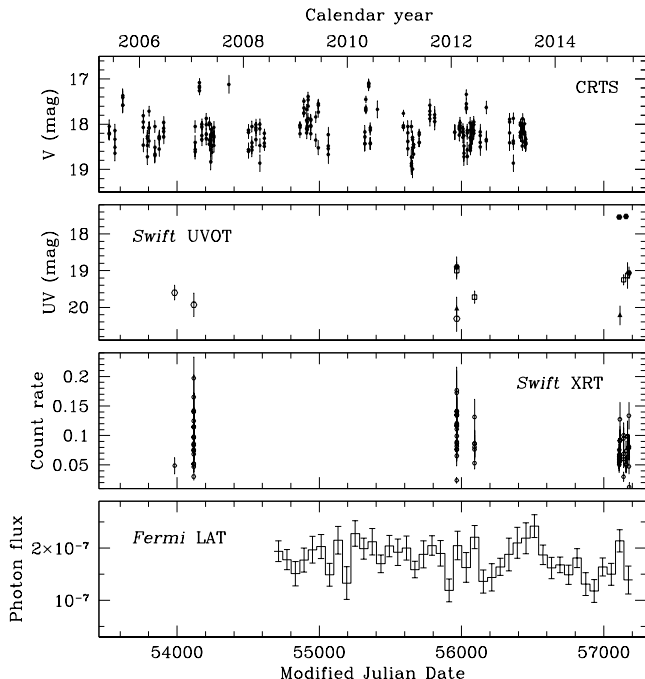


FIG. 3.— Long-term light curves of 1RXS J154439.4–112820 from the Catalina Real-time Transient Survey (CRTS), *Swift* UVOT, *Swift* XRT 0.3–10 keV, and *Fermi* LAT 0.1–100 GeV (from top to bottom, respectively). The different symbols for the *Swift* UVOT data correspond to the various filters: U (solid circles), UVW1 (open squares), UVM2 (open circles), and UVW2 (solid triangles).

data within 20° of the source from the start of the mission on 2008 August 4 through 2015 June 7. The γ -ray light curve was obtained by dividing the data set in 60 day intervals and carrying out a binned likelihood analysis for each time segment using the Fermi Science Tools² v10r0p5. Following the analysis procedures recommended by the Fermi Science Support Center, I first generated counts, exposure, and source maps, livetime cube, and an input source model based on the source information provided in the 3FGL catalog (Acero et al. 2015). In the likelihood fitting with the *gtlike* task, the contribution from all sources within 20° of 1RXS J154439.4–112820, as well as from the Galactic and extragalactic diffuse emission, was taken into account. The best fit values and uncertainties of the flux of 3FGL J1544.6–1125 were used to construct a light curve in the 0.1–100 GeV band.

Although the optical, UV and X-ray data have gaps in coverage spanning several months to years, when combined with the γ -ray data, they provide useful constraints on the long-term behavior of 1RXS J154439.4–112820 within the past decade. For instance, it is apparent that there have been no intervals spanning months to years in which the system has been in a low-flux, non-accreting state. The *Fermi* LAT 0.1–100 GeV light curve shows no appreciable deviations from the mean photon flux of $1.8 \times 10^{-7} \text{ cm}^{-2} \text{ s}^{-1}$. This is consistent with variability index of 47.5 reported for 3FGL J1544.6–1125 in the *Fermi* LAT 4-year catalog (Acero et al. 2015), which indicates no statistically significant flux changes over the course of the mission.

On the other hand, the CRTS and the most re-

cent *Swift* UVOT UVW1 data show instances of enhancement in brightness by $\sim 1 - 1.5$ magnitudes compared to the typical value. These events may correspond to occasional flaring episodes seen from PSR J1023+0038 (Bogdanov et al. 2015) and XSS J12270–4859 (de Martino et al. 2013) in the optical, UV, and X-rays. The *Swift* XRT 0.3–10 keV exposures exhibit large-amplitude variations that span a factor of ~ 10 in count rate. The corresponding range of fluxes are in good agreement with the high and low mode levels observed with *XMM-Newton* (Bogdanov & Halpern 2015).

6. DISCUSSION

The hard X-ray properties of the 1RXS J154439.4–112820 system as revealed by *NuSTAR* are virtually identical to those of the confirmed transitional MSPs. For example, de Martino et al. (2010, 2013) investigated the broad-band X-ray properties of XSS J12270–4859 during its accreting state using data from *XMM-Newton*, *RXTE*, and *INTEGRAL*. The source spectrum in the 0.1–100 keV can be fitted by a single power-law with index $\Gamma \approx 1.7$. In the *RXTE* data, XSS J12270–4859 showed the same mode switching and flaring behavior found in soft X-rays. Tendulkar et al. (2014) presented *NuSTAR* observations of PSR J1023+0038 in both the radio pulsar and accreting X-ray binary states. The average hard X-ray emission in the more luminous accreting state is well-described a power-law with photon index $\Gamma = 1.66$ with a luminosity of $6 \times 10^{33} \text{ erg s}^{-1}$ (3–79 keV). Rapid variability between two clearly separated flux levels was also found.

The available optical/UV, soft and hard X-ray and high-energy γ -ray data for 1RXS J154439.4–112820 allows an examination of the broad-band emission spectrum of the system. Figure 4 shows the optical to GeV γ -ray range for 1RXS J154439.4–112820. For an illustrative comparison, the multi-wavelength data set of PSR J1023+0038 in its accreting state is also shown. The overall similarities in the shape of the broadband spectral energy distributions offers an additional indicator that 1RXS J154439.4–112820 belongs to the same class of objects as PSR J1023+0038, XSS J12270–4859, and PSR J1824–2452I. In light of this, the same interpretations used for these objects can be invoked to explain the different emission components of 1RXS J154439.4–112820. The optical flux is likely a combination of emission from the companion and the accretion disk, with the latter dominating the emission in the UV. The X-ray emission presumably originates in the inner disk, close to or at the surface of the neutron star. The detection of coherent X-ray pulsations during the high mode X-ray emission in PSR J1023+0038 (Archibald et al. 2015) and XSS J12270–4859 (Papitto et al. 2015) and the absence of radio pulsations (Stappers et al. 2014; Bogdanov et al. 2015) suggests that at least during these intervals active accretion onto the stellar surface is taking place and the radio pulsar mechanism is quenched. The cause of the aperiodic rapid drops to a low flux mode is less clear as it may correspond to changes to a propeller ejection process (Illarionov & Sunyaev 1975) or a dead/trapped disk regime (Siuniaevev & Shakura 1977; Spruit & Taam 1993; D’Angelo & Spruit 2010, 2012). Moreover, it is not clear whether the inflow of matter is via a “classical” thin

² Available at <http://fermi.gsfc.nasa.gov/ssc/data/analysis/software/>

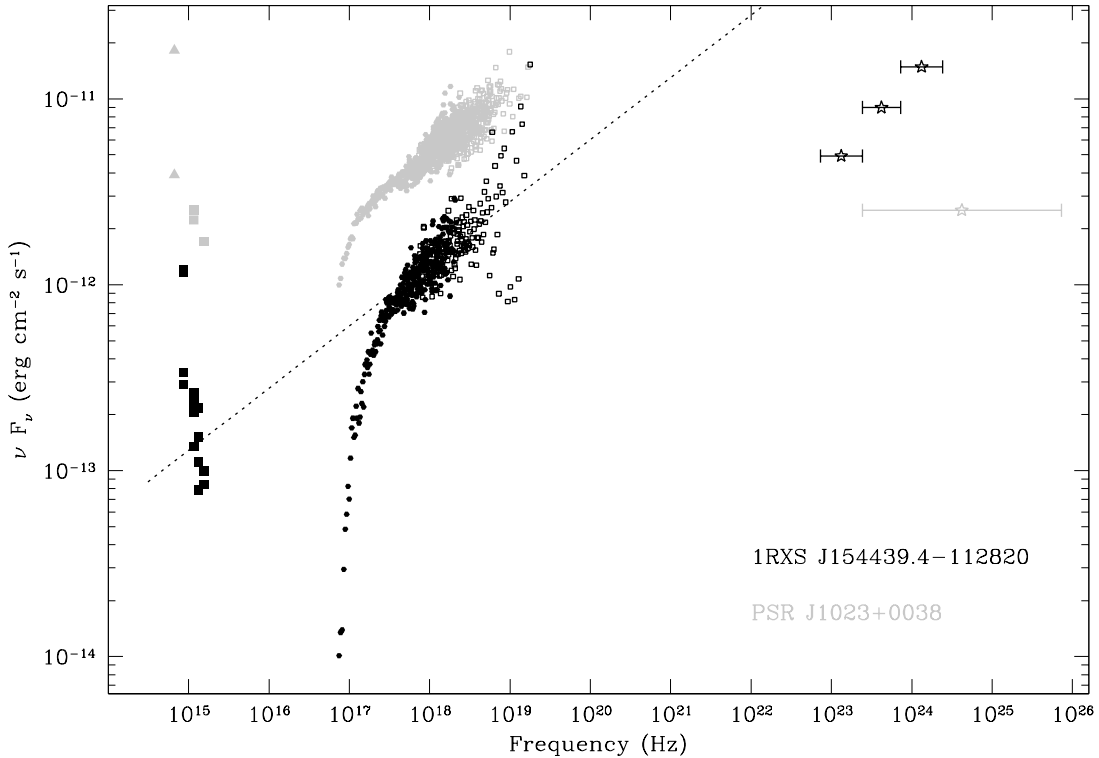


FIG. 4.— The broadband spectrum of 1RXS J154439.4–112820 (black data points) covering the optical to 100 GeV γ -rays range, showing the *Fermi* LAT (open stars), *NuSTAR* (open squares), *XMM-Newton* EPIC (solid circles), *Swift* UVOT (solid squares) and *XMM-Newton* OM B filter (solid triangles). The light grey points correspond to the spectral energy distribution of PSR J1023+0038 (see Bogdanov et al. 2015, for details).

disk or a radiatively inefficient accretion flow (Rees et al. 1982).

The persistent γ -rays from this system possibly arise due up-scattering of X-rays at the boundary between the accretion flow and the neutron star magnetosphere. Two general varieties of models have been put forth to explain the observed γ -rays, which differ principally in the assumption of an active or inactive rotation-powered pulsar wind. In the active pulsar wind scenario, the X-ray and γ -ray emission arise due to an intrabinary shock produced at the interface of the accretion disk and the pulsar wind (Takata et al. 2014; Coti Zelati et al. 2014). The X-rays are generated via synchrotron radiation in the shock, while the γ -rays are the product of inverse Compton scattering of the photons emanating from the accretion disk off the pulsar wind particles. As discussed by (Papitto & Torres 2015), for the case of an inactive (“quenched”) pulsar wind, the system is assumed to be in the so-called propeller regime in which most of the inflowing material is expelled by the rapidly rotating pulsar magnetosphere. The X-ray luminosity is then due to synchrotron plus disk emission, with the flux moding arising from rapid switching between accretion onto the star (the high mode) and propeller ejection (the low mode). The γ -ray emission is produced by synchrotron self-Compton emission by accelerated particles in the turbulent boundary between the pulsar magnetosphere and the accretion disk.

While 1RXS J154439.4–112820 appears to be a close analog of the confirmed transitional MSPs, some notable differences are also apparent. In particular, the γ -ray flux of 1RXS J154439.4–112820 is ~ 3 higher than that

of PSR J1023+0038, whereas the mean X-ray flux is ~ 3 times lower. While the lower X-ray flux can be attributed to a greater distance (assuming a comparable intrinsic luminosity), the relative differences in X-ray to γ -ray flux may arise either due to higher efficiency of the γ -ray production mechanism or due to a more favorable viewing angle if the radiation pattern is not isotropic. In addition, for PSR J1023+0038, the high and low mode X-ray fluxes differ by a factor of ≈ 6 , while for 1RXS J154439.4–112820 the flux varies by a factor of ≈ 10 . Assuming that during the low X-ray mode, the accretion flow is cleared out of the pulsar magnetosphere, this difference could be ascribed to a larger accretion disk truncation radius in 1RXS J154439.4–112820. If this radius coincides with the pulsar light cylinder ($cP/2\pi$) it implies a more slowly spinning neutron star, although other factors like a less massive neutron star or a different magnetic field configuration may play a role in determining the high/low flux ratio.

7. CONCLUSIONS

I have presented the first hard X-ray observation of the low-luminosity X-ray binary and *Fermi* LAT source, 1RXS J154439.4–112820 / 3GL J1544.6–1125. The binary is detected at high significance up to ~ 30 keV with a continuation of the power-law spectrum observed in soft X-rays. The hard X-rays also exhibit variability on timescales of 10–100 seconds by a factor of ≈ 10 in flux as seen in the 0.3–10 keV range with *XMM-Newton*. The spectral energy distribution of 1RXS J154439.4–112820 covering the optical through GeV range is qualitatively very similar to that of PSR J1023+0038 (as well as

XSS J12270–4859; see de Martino et al. 2010, 2013). These findings further strengthen the argument that this system belongs to the same class of objects as PSR J1023+0038, XSS J12270–4859 and PSR J1824–24I, namely a compact binary hosting a MSP that is presently accreting at low luminosities.

I find no clear evidence in archival data for prolonged low flux intervals at any wavelength implying that within the past \sim decade 1RXS J154439.4–112820 has most likely not experienced a transformation to a disk-free state. Nevertheless, as the strongest transitional MSP candidate, 1RXS J154439.4–112820 warrants dedicated monitoring to identify behavior that may signal the disappearance of its accretion disk and the activation of the

rotation-powered millisecond pulsar.

I thank F. Harrison for approving the DDT request that enabled the *NuSTAR* observation. This work is based on data from the *NuSTAR* mission, a project led by the California Institute of Technology, managed by the Jet Propulsion Laboratory, and funded by NASA. I thank the *NuSTAR* Operations, Software and Calibration teams for support with the execution and analysis of these observations. This research has made use of the *NuSTAR* Data Analysis Software (NuSTARDAS) jointly developed by the ASI Science Data Center (ASDC, Italy) and the California Institute of Technology (USA), the arXiv, NASA ADS, and data and software facilities from the Fermi Science Support Center, managed by the HEASARC at NASA GSFC.

REFERENCES

- Acero, F., Ackermann, M., Ajello, M., et al. 2015, *ApJS*, 218, 23
 Archibald, A. M., Bogdanov, S., Patruno, A., et al. 2015, *ApJ*, 807, 62
 Arnaud, K. A. 1996, in *ASP Conf. Ser. 101, Astronomical Data Analysis Software and Systems V*, ed. G. H. Jacoby & J. Barnes (San Francisco, CA: ASP), 17
 Bassa, C. G., Patruno, A., Hessels, J. W. T., et al. 2014, *MNRAS*, 441, 1825
 Becker, W., Swartz, D. A., Pavlov, G. G., et al. 2003, *ApJ*, 594, 798
 Bogdanov, S., Patruno, A., Archibald, A. M., et al. 2014a, *ApJ*, 789, 40
 Bogdanov, S., Archibald, A., Bassa, C., et al. 2015, *ApJ*, 806, 148
 Bogdanov, S., & Halpern, J. P. 2015, *ApJ*, 803, L27
 Bogdanov, S., van den Berg, M., Servillat, M., et al. 2011, 730, 81
 Chakrabarty, D., Tomsick, J. A., Grefenstette, B. W., et al. 2014, *ApJ*, 797, 92
 Coti Zelati, F., Baglio, M. C., Campana, S., et al. 2014, *MNRAS*, 444, 1783
 D’Angelo, C. R., & H. C. Spruit H. C. 2010, *MNRAS*, 406, 1208
 D’Angelo, C. R., & H. C. Spruit H. 2012, *MNRAS*, 420, 416
 Deller, A. T., Moldon, J., Miller-Jones, J. C. A., et al., 2015, *ApJ*, 809, 13
 de Martino, D., Belloni, T., Falanga, M., et al. 2013, *A&A*, 550, 89
 de Martino, D., Falanga, M., Bonnet-Bidaud, et al. 2010, *A&A*, 515, 25
 Drake, A. J., Djorgovski, S. G., Mahabal, A., et al. 2009, *ApJ*, 696, 870
 Harrison, F. A., Craig, W. W., Christensen, F. E., et al. 2013, *ApJ*, 770, 103
 Hill, A. B., Szostek, A., Corbel, S., et al. 2011, *MNRAS*, 415, 235
 Illarionov, A. F., & Sunyaev, R. A. 1975, *A&A*, 39, 185
 Linares, M., Bahramian, A., Heinke, C., et al. 2014, *MNRAS*, 438, 251
 Masetti, N., Sbarufatti, B., Parisi, P., et al. 2013, *A&A*, 559, A58
 Pallanca, C., Dalessandro, E., Ferraro, F. R., Lanzoni, B., & Beccari, G. 2013, *ApJ*, 773, 122
 Papitto, A., Ferrigno, C., Bozzo, E., et al. 2013, *Nature*, 501, 517
 Papitto, A., Torres, D. F., & Li, J. 2014, *MNRAS*, 438, 2105
 Papitto, A., de Martino, D., Belloni, T. M., et al. 2015, *MNRAS*, 449, L26
 Papitto, A., & Torres, D. F. 2015, *ApJ*, 807, 33
 Patruno, A., Archibald, A. M., Hessels, J. W. T., et al. 2014, *ApJ*, 781, L3
 Rees, M. J., Begelman, M. C., Blandford, R. D., & Phinney, E. S., 1982, *Nature*, 295, 17
 Roy, J., Ray, P. S., Bhattacharyya, B., et al. 2015, *ApJ*, 800, L12
 Siuniae, R. A., & Shakura, N. I. 1977, *PAZh*, 3, 262
 Spruit, H. C., & Taam, R. E. 1993, *ApJ*, 402, 593
 Stappers, B. W., Archibald, A. M., Hessels, J. W. T., et al. 2014, *ApJ*, 790, 39
 Stephen, J. B., Bassani, L., Landi, R., Malizia, A., Sguera, V., Bazzano, A., Masetti, N. 2010, *MNRAS*, 408, 422
 Takata, J., Li, K. L., Leung, G. C. K., 2014, *ApJ*, 785, 131
 Tendulkar, S. P., Yang, C., An, H., et al. 2014, *ApJ*, 791, 77
 Yi, X., & Wang, Z. 2015, *ApJ*, 808, 17
 Wilms, J., Allen, A., & McCray, R. 2000, *ApJ*, 542, 914